

**Supplemental Table 1. In situ tetramer staining results in lymph nodes and spleens of rhesus macaques<sup>a</sup>.**

Animal	Tissue site	Mamu-A1*001:01		Mamu-A1*002:01 Nef YY9 YTSGPGIRY	Mamu-B*008:01			
		Gag CM9 CTPYDINQM	Tat SL8 STPESANL		Vif RL8 RRDNRRL	Vif RL9 RRAIRGEQL	Nef RL10 RRHRILDIYL	Env KL9 KROQELLRL
Rh2306	Spleen	+ <sup>b</sup>	- <sup>c</sup>					
	Inguinal LN	+	-					
	Axillary LN	+	-					
	Meso-colonic LN	+	-					
	Mesenteric LN	+* <sup>d</sup>	-					
	Trachial Bronch LN	+*	-					
R03116	Spleen	+	-					
	Inguinal LN	+*	+					
	Axillary LN	+*	-					
	Mesenteric LN	+*	-					
	Meso-colonic LN	+*	-					
Rh2123	Spleen	+						
	Inguinal LN	+						
R03094	Inguinal LN	+	-					
R03111	Inguinal LN			+*				
	Axillary LN			+				
Rhau10	Spleen						+	
	Inguinal LN				+	+	+	
	Mesenteric LN				+*	+	+	+
	Ileum				-	+*	+*	
Rhax18	Spleen						+	
	Axillary LN					+	+	
	Iliac LN						+	
	Ileum						+*	
R01106	Spleen							+
	Inguinal LN				+*	+		+
	Axillary LN							+
	Mesenteric LN					+	+	+
	Iliac LN				-	+*		+
	Ileum							+*

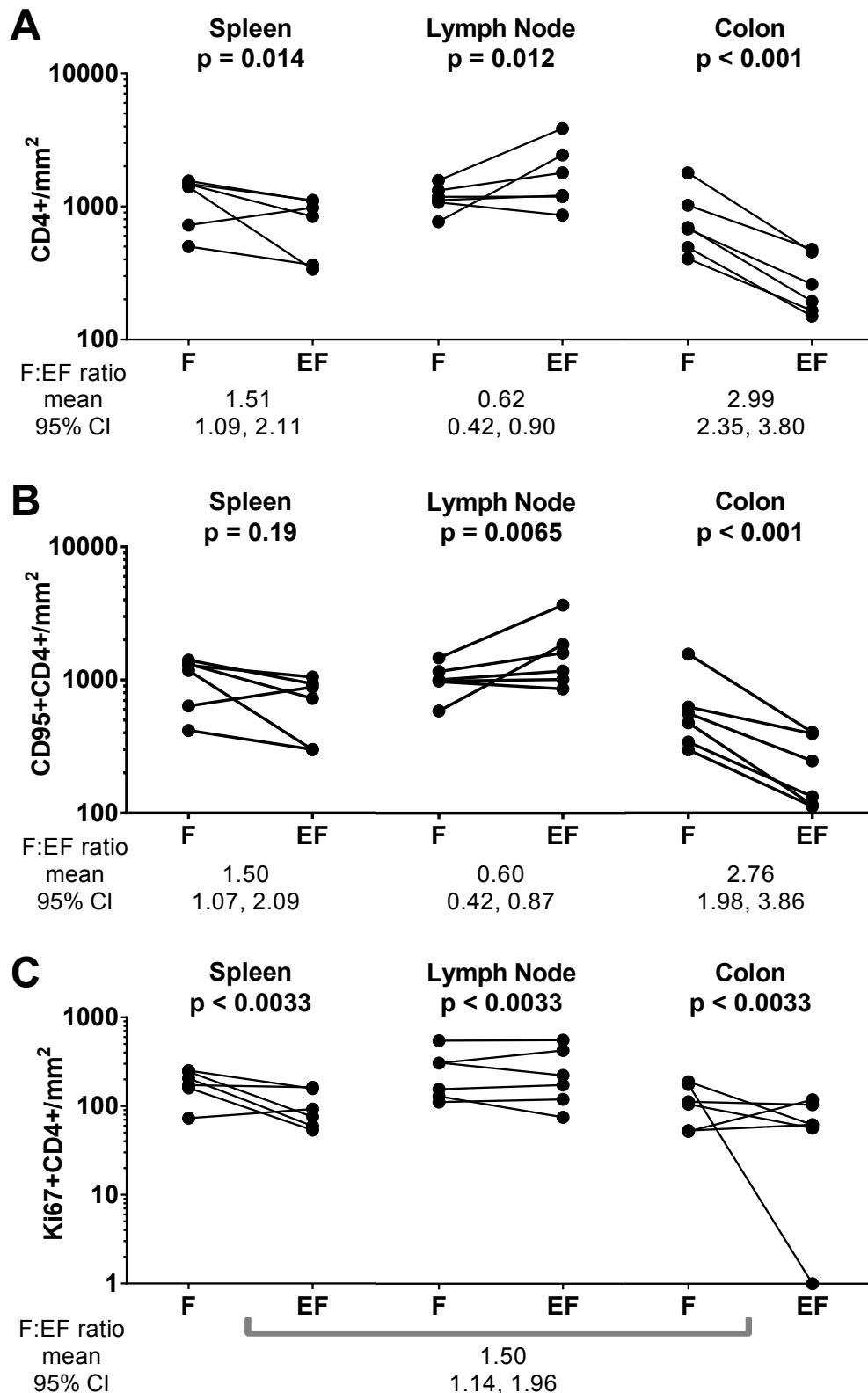
<sup>a</sup> Shaded boxes indicate tissue was not stained or stained tissues were not evaluated.

<sup>b</sup> + indicates that tetramer+ cells were detected above background levels in controls.

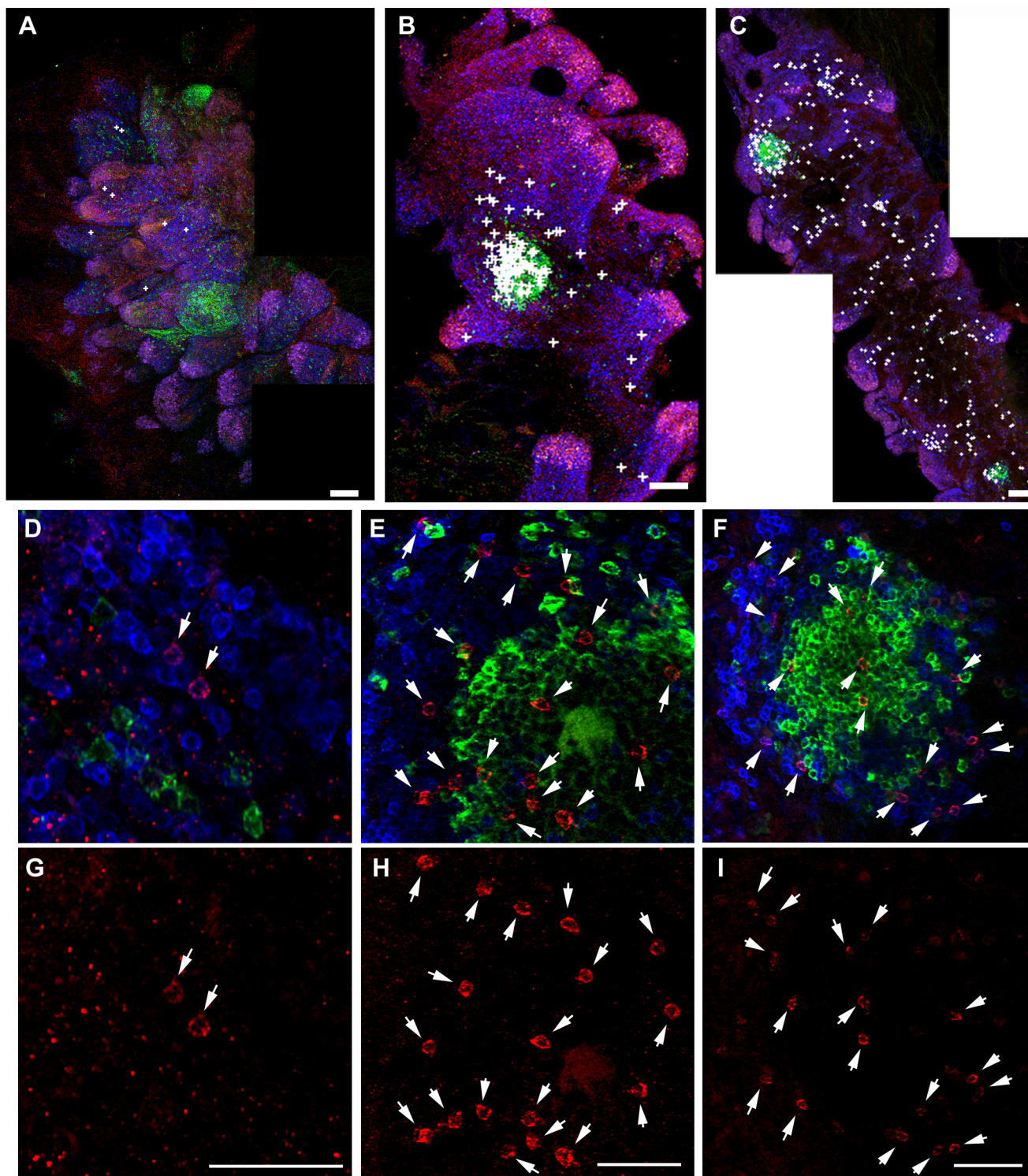
<sup>c</sup> - indicates few or no tetramer+ cells were detected above background levels in controls.

<sup>d</sup> \* indicates that tetramer+ cells were not quantified due to detection of <3 follicles or time constraints.

Supplemental Figure 1

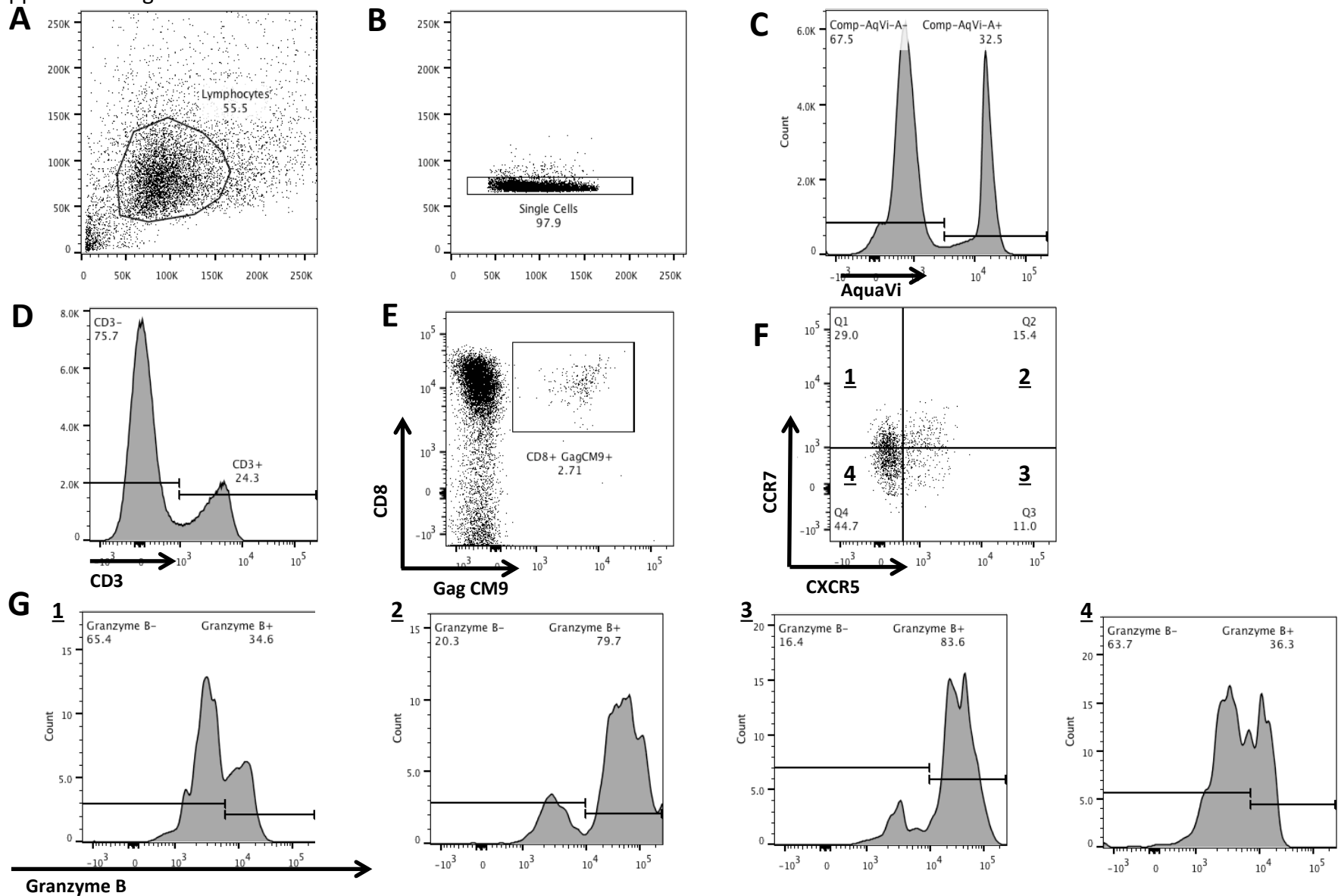


**Supplemental Figure 1. Distribution of CD4+ cells (A), CD95+CD4+ cells (B), and Ki67+ CD4+ cells (C) in secondary lymphoid tissue compartments of chronically SIV-infected rhesus macaques.** Tissues were stained with immunofluorescent antibodies and numbers of CD4+ cells, CD95+CD4+ cells, and Ki67+ CD4+ cells determined by visual inspection and quantitative image analysis. Data were analyzed using a generalized linear model for a negative binomial distribution that accounted for within animal correlation and adjusted for  $\log_e$  (area). The F:EF ratio of CD4+ cells and CD4+CD95+ cells varied significantly by tissue ( $p < 0.0001$  in both instances). The F:EF ratio of Ki67+CD4+ cells did not vary significantly by tissue ( $p = 0.10$ ).



Supplemental Figure 2. Localization of SIV-specific CTL in ileum of rhesus macaques during chronic infection. Representative ileum tissue sections stained with MHC class I tetramers (red) to label SIV-specific CTL, CD3 antibodies (blue) to label T cells, and CD20 antibodies (green) to label B cells and delineate B cell follicles. Panels (A-C) show montages of multiple confocal projected serial z-scans from ileum. Tetramer+ cells within the sections were identified in montages of high-resolution serial z-scans, and are indicated by white crosses. (A) Macaque Rhau10 and (B) macaque Rhax19 ileum sections stained with Mamu-B\*008:01/Nef RL10 tetramers. (C) Macaque R01106 (which had SAIDS) ileum section stained with Mamu B\*008:01/Env KL9 tetramers. Panels D-F show enlarged confocal z-scans from areas within the corresponding sections presented in panels A-C. Below, panels G-I show the red (tetramer) staining alone (arrows), from each of the corresponding images above. Confocal images were collected with a 20X objective and scale bars indicate 100  $\mu$ m in panels A-C, and 50  $\mu$ m in G-I.

Supplemental Figure 3



**Supplemental Figure 3. Representative flow cytometry plots demonstrating the gating strategy to determine CXCR5, CCR7, and granzyme B expression in SIV-specific CTL.** Multi-parameter flow cytometry was utilized to analyze disaggregated lymphocytes (A) from lymph nodes and spleen of rhesus macaques. Only single cells (B) that were viable (AquaVi-) (C) were analyzed. SIV-specific cells were defined as CD3+ (D) and CD8+tetramer+ (E). SIV-specific CTL were then assessed for CCR7 and CXCR5 expression (F) and the level of granzyme B on each subset (quadrants 1-4) was determined (G).